IIETA International Information and Engineering Technology Association
Advancing the World of Information and Engineering

Annales de Chimie - Science des Matériaux
Vol. 49, No. 3, June, 2025, pp. 261-269
Journal homepage: http://iieta.org/journals/acsm

Selective Removal of Nitrophenols from Aqueous Solutions Using Acrylic Acid–Acrylamide Molecularly Imprinted Polymers

Ibtehal Habib Al Rashid, Ibrahim M. Al-Naiema*, Salah Shakir Hashim

Department of Chemistry Sciences, University of Basrah, Basrah 61004, Iraq

Corresponding Author Email: ibrahim.jasim@uobasrah.edu.iq

https://doi.org/10.18280/acsm.490305

Received: 17 May 2025
Revised: 18 June 2025
Accepted: 22 June 2025
Available online: 30 June 2025

Keywords:
nitrophenol removal, selective adsorption, water pollution, extraction efficiency, molecular imprinting polymer, acrylic acid, acrylic amide

ABSTRACT

Nitrophenols are environmentally persistent and toxic pollutants of global concern due to their harmful effects on ecosystems and human health. This study presents the synthesis of molecularly imprinted polymers (MIPs) based on poly (acrylic acid-co-acrylamide) [PAA-co-PAAm], for the selective extraction of nitrophenol isomers from aqueous media for the first time. Characterization by FT-IR, TGA, and UV–Vis spectroscopy confirmed successful incorporation of cross-linking functionalities and enhanced structural integrity in MIPs compared to non-imprinted polymers (NIPs). Extraction efficiency was evaluated by determining the distribution ratio (D) of ortho-, meta-, and para-nitrophenol at pH 2, 7, and 10. D values increased with decreasing pH, with meta-nitrophenol (MNP) showing the highest selectivity. At pH 2, the D for MNP reached 4.6, a sevenfold increase over its value at pH 7. Among the three isomers studied, the MIP synthesized for MNP showed the highest binding efficiency and imprinting factor (I.F.), likely due to the formation of highly specific hydrogen-bonding interactions. Selectivity tests further confirmed the superior recognition of MNP by the MIPs compared to structurally similar compounds such as phenol and m-cresol. These results highlight the potential of PAA-co-PAAm–based MIPs as effective and selective adsorbents for the removal of nitrophenol isomers from contaminated water sources.

1. INTRODUCTION

Nitrophenol isomers are hazardous aromatic compounds that their toxicity, solubility, acidity, and environmental behavior are largely dictated by the different position of the nitro and hydroxyl group [1]. Of which, PNP is the most environmentally persistent and toxic, commonly entering aquatic systems through the breakdown of pesticides [2], industrial production [3], fossil fuel combustion [4], and biomass burning [5]. Nitrophenols have been detected in surface waters at levels ranged from nanograms to a few micrograms per liter, mostly near industrial and agricultural regions [3]. Toxicity data indicate that PNP is especially harmful to aquatic life [6], and human. These compounds classified by GHS as toxic by inhalation, ingestion, or dermal contact and capable of causing serious eye damage, skin irritation, and organ toxicity with repeated exposure [3]. Moreover, nitrophenols can impair cellular functions, induce oxidative stress, and may act as endocrine disruptors, raising environmental concerns due to their ability to persist and accumulate in ecosystems [7].

Pollutant removal from aqueous solutions involves techniques such as adsorption, membrane filtration, advanced oxidation processes, biological treatment, and electrochemical methods, each suited to specific contaminants like heavy metals, organics, or pathogens [8, 9]. While methods like adsorption and advanced oxidation processes offer high efficiency, challenges such as cost, and limited selectivity affect their large-scale applicability [10]. Molecular imprinting is a technique used to create synthetic polymers with highly specific recognition sites for a target molecule, known as the template [11]. During the process, functional monomers form a complex with the template molecule, and this complex is polymerized in the presence of a cross-linker to form a rigid matrix. After polymerization, the template is removed, leaving behind cavities that are complementary in size, shape, and functional groups to the original molecule [11]. These cavities enable the polymer, known as a molecularly imprinted polymer (MIP), to selectively rebind the target molecule with high affinity. Compared to conventional adsorbents, MIPs offer significant advantages in terms of selectivity and efficiency [12]. While conventional materials rely on non-specific interactions and typically exhibit broad-range adsorption, MIPs provide highly specific recognition due to their tailor-made binding sites [13]. These characteristics make MIPs particularly useful in applications such as sensors, drug delivery, solid-phase extraction, chromatography, and environmental monitoring, where selective and efficient molecule targeting is essential.

Several studies have demonstrated the effectiveness of molecularly imprinted polymers (MIPs) for the selective removal of nitrophenol compounds from aqueous solutions. A

cellulose-based MIP grafted with DMAEMA showed high affinity for PNP, achieving an adsorption capacity of 26.9 mg/g and strong selectivity over structurally similar compounds like MNP and catechol [14]. Similarly, a MIP synthesized with acrylamide for 2,4-dinitrophenol exhibited favorable adsorption isotherms and high selectivity in the presence of phenol derivatives [15]. Another study has investigated enhancing surface area and accessibility, silica-coated MIP nanoparticles for PNP extraction from pharmaceutical samples, displaying improved binding and rapid adsorption [16]. Meanwhile, magnetic MIPs based on Fe_3O_4 functionalized nanoparticles achieved a high adsorption capacity (129 mg/g) within 90 minutes PNP and allowed for magnetic recovery, which simplifies separation processes [17]. Additionally, early work using methacrylamidoantipyrine (MAAP) as a functional monomer demonstrated that π–π interactions and hydrogen bonding could markedly improve binding strength, with adsorption capacities surpassing traditional MAA-based MIPs [18]. Together, these studies illustrate a clear trend toward surface-imprinted, magnetically responsive, and multi-target MIPs, addressing key limitations in selectivity, kinetics, and operational practicality for nitrophenol removal

In this study, we investigate the selective removal of specific nitrophenol isomers from aqueous solution using Acrylic Acid–Acrylamide MIP, for the first time. In addition to the selectivity, we have assessed the thermal stability and extraction efficiency under different pH condition, which are relevant to industrial waste water. Overall, the outcome of this research provides a practical approach to selectively remove nitrophenol form aqueous solution, specifically in industrial and anthropogenically-influenced environments.

2. EXPERIMENTAL WORK

Figure 1 shows schematic diagram of the preparation steps of MIP for nitrophenols isomers.

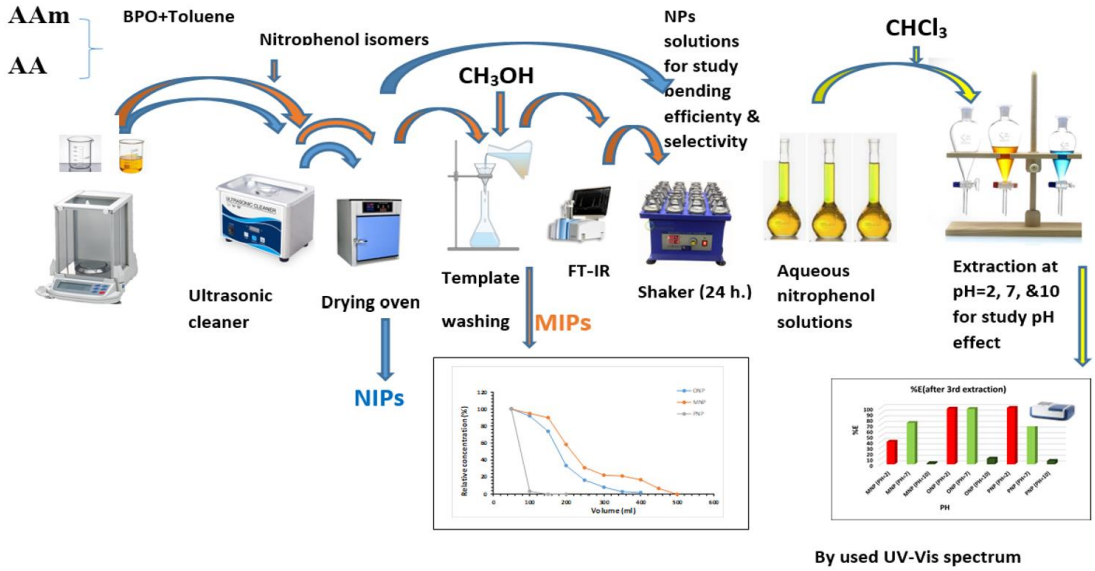

Figure 1. Schematic diagram of the preparation steps of MIP for nitrophenols isomers

2.1 Materials

The monomer that used in this study was an acrylamide (AAm), (C_3H_5NO) was acquired from Merck and acrylic acid (AA), ($C_3H_4O_2$, 90%) from CDH. They were used as supplied. N, N-'methylene bisacrylamide (MBA) as crosslinking from CDH supplying source ($C_7H_{10}N_2O_2$). Three nitrophenol isomers ($C_6H_5NO_3$) from BDH origin. Benzoyl peroxide ($C_{14}H_{10}O_4$) was used as initiator from Merck (BPO). Chloroform ($CHCl_3$) from Merck. Analytical-grade chemicals were used for all experiments. Hydrochloric acid (HCl, 99%) was acquired from GCC, and sodium hydroxide (NaOH, 99%) was acquired from Merck. Methanol (CH_3OH, 99.5%) and toluene (C7H8, 99.5%) were acquired from SDFCL.

2.2 Preparation of MIPS and NIPs

MIPs were synthesized by combining 2 ml of AA, and 2 g of AAm, 0.8 g of MBA, and 0.2 g of a selected nitrophenol isomer either ONP, PNP, or MNP in 40 ml of toluene [19]. The resulting mixture was sonicated for 30 minutes to ensure homogeneity [20]. Subsequently, 0.4 g of BPO, previously dissolved in 10 ml of toluene, was added as the initiator. Copolymerization was conducted at a temperature range of 70–78°C under continuous stirring for 1 hr until the formation of the copolymer was complete. The resulting it was then dried in an oven at 70°C for 5 h. This procedure was repeated for each nitrophenol isomer (*ortho*, *para* and *meta*) to yield three distinct MIPs. A NIP was synthesized under identical conditions, excluding the addition of the nitrophenol template, as Schemes 1 and 2.

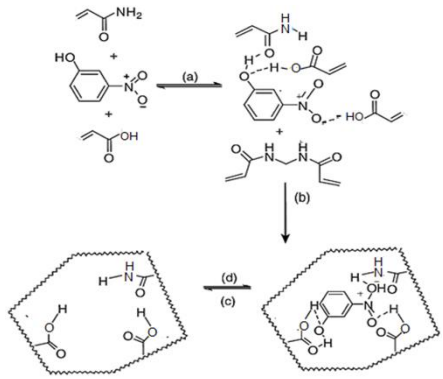

Scheme 1. MIPs poly (AA-*co*-AAm) for MNP

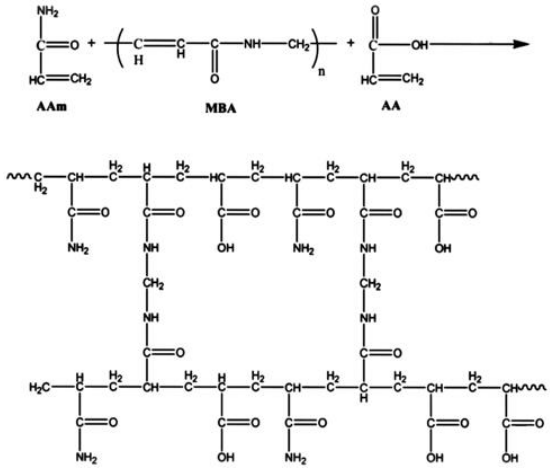

Scheme 2. Cross-linked Poly (AA-*co*-AAm)

2.3 Template removal from MIPs

The nitrophenol were removed from the template by repeated washing of the polymers with 50 ml aliquots of methanol in an ultrasonic water bath, with each cycle lasting 30 minutes. The efficiency of the template removal process was monitored by analyzing the filtrates for residual nitrophenol. Washing was continued until no detectable concentration of the template was observed using UV spectroscopy, thereby confirming complete removal.

2.4 Calibration curve of nitrophenols

The λ_{max} measurements in aqueous solution are shown in Figure 2, and indicated that λ_{max} of the prepared standards in aqueous solution were 378, 404, 400 nm for *ortho, meta* and *para* nitrophenols, respectively. While the λ_{max} measurements for the nitrophenols prepared in chloroform solution were 350, 326, and 316 nm for *ortho, meta* and *para* isomers, as shown in Figure 3.

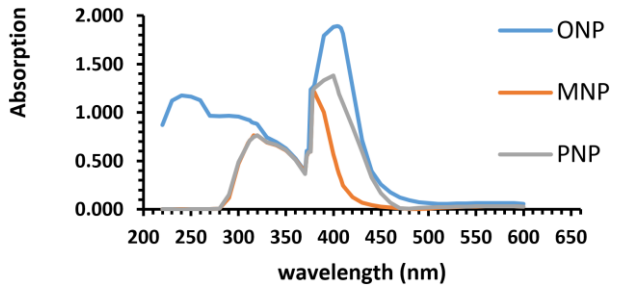

Figure 2. UV spectrum of nitrophenols in aqueous solution

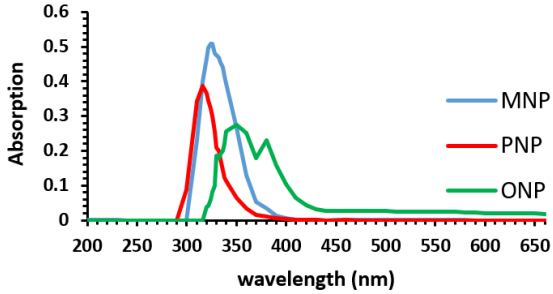

Figure 3. UV spectrum of nitrophenols in chloroform solution

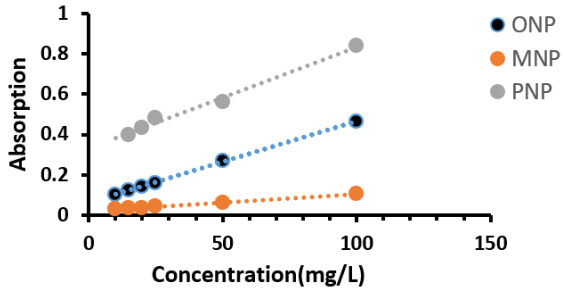

Figure 4. Calibration curve for nitrophenol isomers in the aqueous solution

Figure 4 shown the standard calibration curves for each of the nitrophenol were examined by preparing concentrations of 10, 15, 20, 25, 50, and 100 mg L^{-1} from 100 mg L^{-1} stock solution for each of the three solutions (ONP, MNP and PNP) in aqueous solutions. As in aqueous solutions the standard calibration curves for each of the nitrophenol in chloroform shown in Figure 5 were examined by preparing different concentrations of 5, 10, 15, 20, and 25 mg L^{-1} except for MNP, where the linear range of the calibration curve was ranged 10 to 50 mg L^{-1} from 100 mg L^{-1} stock solution.

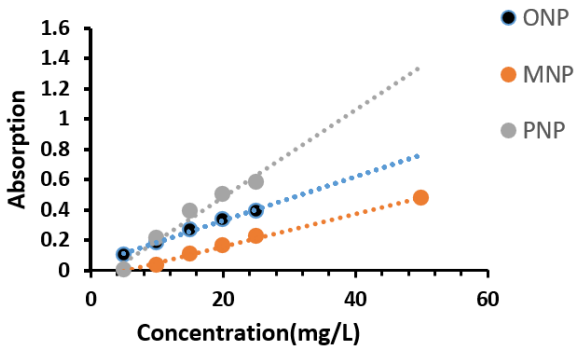

Figure 5. Calibration curve for nitrophenol isomers in the chloroform solution

2.5 pH study

The pKa of the three nitrophenol isomers ranges 7.19 – 8.1. Thus, we have tested the extraction efficiency of nitrophenol from water at pH values lower and higher than the pKa to test the impact of ionization on the extraction from water to chloroform. The pH adjustment process involved adding drops from diluted acid (HCl), and base (NaOH) with continuous monitoring to the value of pH using pH meter. Therefore, two standard solutions of NaOH and HCl (0.1 N) were used to study the effect of the pH on the efficiency of the extraction. 0.1 M solutions.

3. RESULTS AND DISCUSSION

The FT-IR spectra of poly (AA-*co*-AAm) and its MIP are shown in Figures 6 and 7, respectively. The Figures showed a broad absorption band at (3000-3700) cm^{-1}, which corresponds to OH vibrations and NH stretching bands, indicating the presence of hydroxyl and amide groups [21, 22].

The frequency Peak at (1670-1675) cm^{-1} is attributed to the carbonyl group C=O of the acrylamide functional group, which may shift slightly during polymerization [21, 22], while peak at (1630-1650) cm^{-1} was associated with the C=O

stretching of the carboxylate groups of acrylic acid [21, 22]. Additionally, the peak at (2938-2949) cm^{-1} was attributed to C-H stretching vibrations of the main chain of polyme [22, 23].

For MIP of copolymer, peak at 1724 cm^{-1} was attributed to stretching carbonyl of carboxylic acid groups in acrylic acid units, while the peak at 1670 cm^{-1} corresponds to the carbonyl stretching of the carbetamide groups in acrylamide units. These data are in good agreement with common carbonyl stretching (C=O) peaks that are generally observed around 1724 cm^{-1} and 1670 cm^{-1} [24, 25].

Peaks around 2924 cm^{-1} are due to stretching vibrations C-H in the main chain of polymer [24]. Also, a wide band between (3000-3700) cm^{-1} corresponds to vibrations OH and NH stretching, indicating the presence of hydroxyl groups of acrylic acid and amine groups of acrylamide [21]. The important peaks in IR spectrum are listed in Table 1 match to those previously published [21-25].

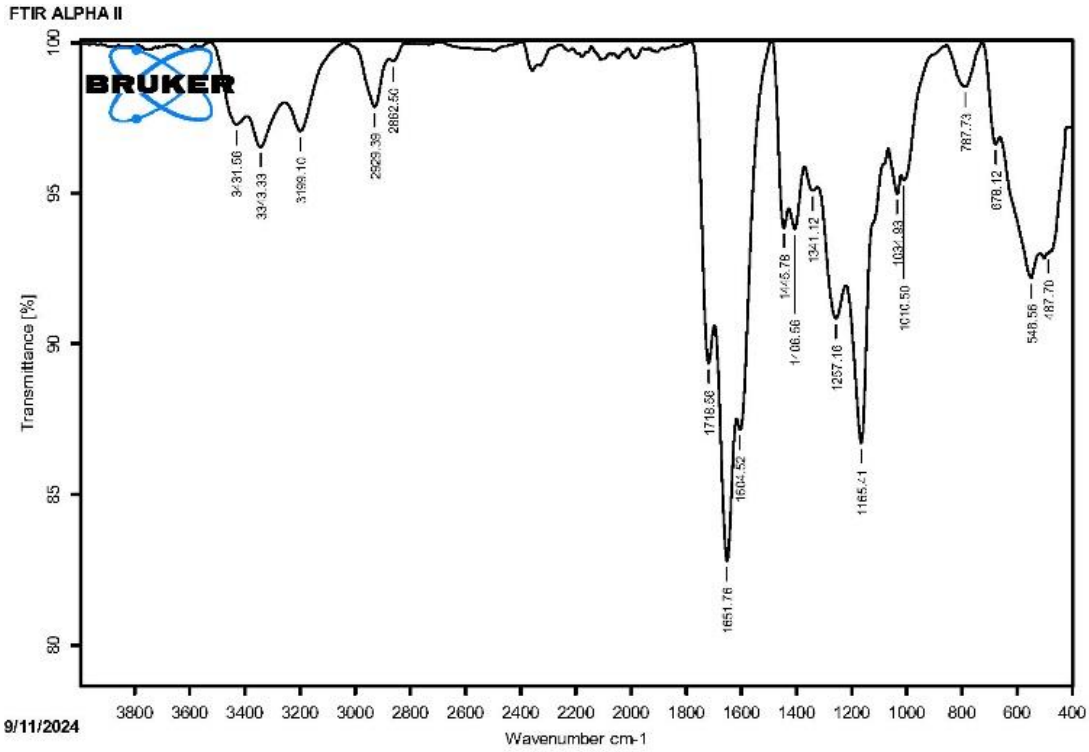

Figure 6. FT-IR spectrum of copolymer

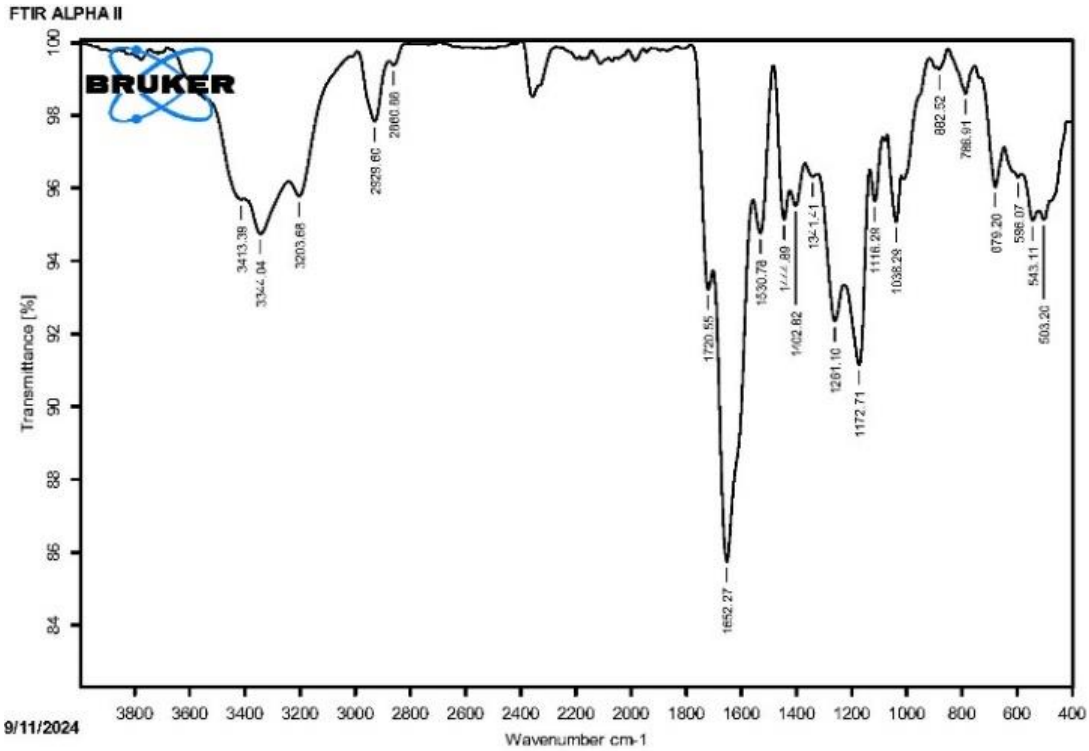

Figure 7. FT-IR spectrum of MIP

Table 1. The important IR bands of copolymer (Co.) and its MIP

Functional Groups	Wavenumber of Peak cm^{-1}	
	Co.	MIP
O-H and N-H stretching vibrations	3199-3432	3203-3413
C=O of acrylamide	1652	1653
C=O of acrylic acid	1719	1721
Amide (-(C=O)-NH -)	-	1531
C-N stretching vibration of amide group	1446	1445
Aliphatic (C-H) stretching vibrations	2929	2930
Symmetrical stretching of anion carboxylate	1407	1403
C-O stretching interaction	1035	1038

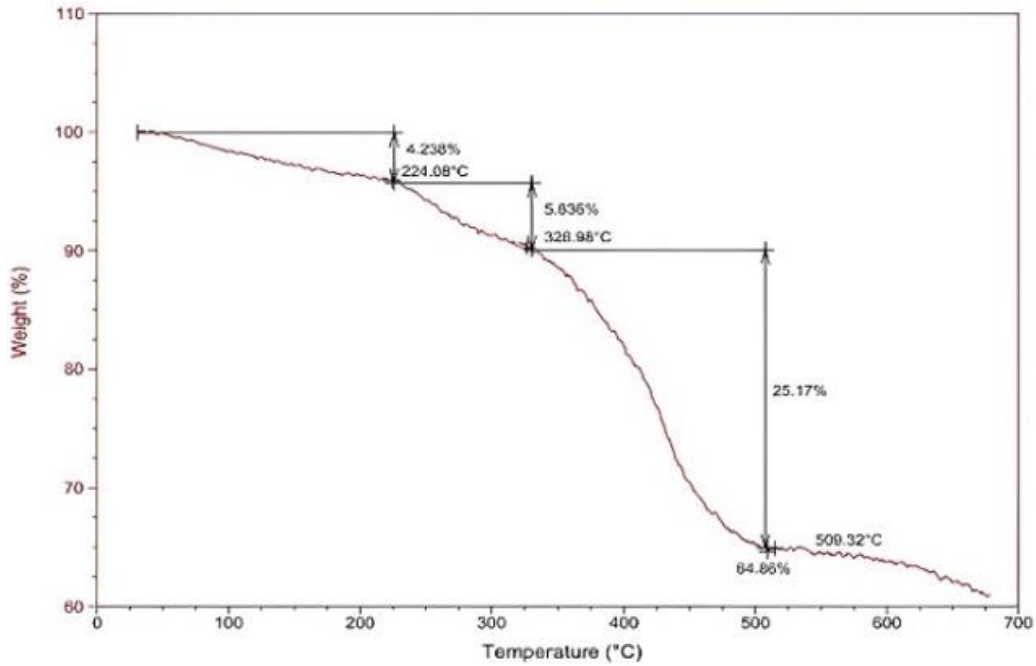

Figure 8. TGA Thermogram of MIP

Table 2. Evaluation of the rebinding efficiency (%E) for the nitrophenol isomers

Polymer	%E	C_i (mg L^{-1})	C_f (mg L^{-1})	S_b (mg L^{-1})	S_b,g	K_p ($*10^{-3}$)	I.F.	ΔG (J $mole^{-1}$)
MIP *ONP*	17.193	15.0	12.421	2.579	0.013	1.047	1.214	169.720
NIP *ONP*	14.893	15.0	12.766	2.234	0.011	0.862	-	174.529
MIP *MNP*	12.7	15.0	13.1	1.89	0.090	0.687	-	180.142
NIP *MNP*	0.0	15.0	15.0	0.00	0.000	0.000	-	-
MIP *PNP*	16.067	15.0	12.590	2.410	0.012	0.953	14.017	172.047
NIP *PNP*	1.247	15.0	14.813	0.187	0.001	0.068	-	237.348

Figure 8 is shown the TGA Thermogram of MIP for copolymer. Its, shows a 4.2% initial weight loss between 25℃ and 224.1℃. The decomposition proceeds in three stages: 5.6% weight loss between 224.1℃ and 327℃, followed by a 25.2% loss from 327℃ to 509.3℃. The char content is relatively high 60%, and the maximum decomposition rate is the lowest among the three 2.9%/min, indicating enhanced thermal stability, likely due to the synergistic effect of the copolymer composition.

Figures 9 shows the relative percentage of the remained nitrophenol isomers as a function to the volume of methanol used to rinse the template (50 ml portion of methanol each time using an ultrasonic water bath for 30 min). The reduction percentage of the initial concentration in of nitrophenol present in the template was tracked until the no more analyte was detected.

It was noted that the both of ONP and MNP needed 400 and 500 ml of methanol respectively to be completely removed from the copolymer template, unlike PNP which was completely removed using 150 ml. This behavior likely associated with the more intramolecular interaction (hydrogen bonding) of the ONP compared to PNP [26, 27], increasing its binding to the active sites, delaying its removal from the template. Thus, less time, sonication, and volume of methanol are needed to remove PNP from the template compares to the other studied isomers (*ortho* and *meta*).

Table 2 summarizes the results obtained in this study. The rebinding efficiency of the three prepared MIPs with the copolymer studied was evaluated. The evaluation study was performed used spectrophotometry.

The results summarized in the above table indicate that the cross-linker, MBA, plays a crucial role in the binding of

template molecules. The presence of the functional group (-CO-NH-CH_2-NH-CO-) in the cross-linker likely contributes significantly to the enhancement of binding efficiency, therefore %E of MIP is higher than %E of NIP [20].

Copolymer-based MIPs can be attributed to the specific nature and strength of interactions formed between the template molecule MNP and the functional monomers during the imprinting process.

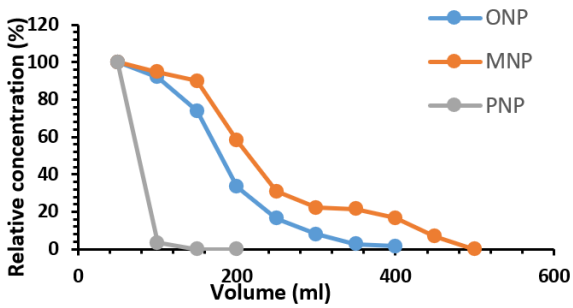

Figure 9. Removal (%) of nitrophenol isomers from the Co. templates

Copolymerization plays important role in the efficiency of rebinding. The use of copolymers in molecular imprinting can diminish the specificity of interactions between the functional monomer and the template molecule. The incorporation of multiple monomer types may dilute these specific interactions, resulting in reduced formation of well-defined binding sites. Additionally, the structural heterogeneity introduced through copolymerization can disrupt the optimal spatial arrangement necessary for high-affinity binding, ultimately leading to decreased binding efficiency for MNP [28].

In contrast, cross-linked copolymer-based MIPs often exhibit reduced binding efficiency due to increased compositional complexity, which can disrupt optimal binding site formation and weaken template recognition [28, 29].

***The initial concentration (C_i):** It represents a concentration of 15 mg L^{-1}, which are nitrophenol solutions that were previously prepared with chloroform. Polymers prepared with chloroform solvent dissolve to a high degree because it is a solvent with weak hydrogen bonding [30, 31].

***The final concentration (C_f):** It is the concentration of the filtrate measured in milligrams per liter of the original solution after 24 hours of placing the sample in it.

***Moles of substrate bound per gram of polymer (S_b):** It is calculated from the following two relationships [30]:

$$S_b = C_i - C_f \quad (1)$$

$$S_b, g = S_b / W_p \quad (2)$$

***The partition coefficient (K_p):** is the partition coefficient of substrate on the MIP divided by the substrate in solution [30]:

$$K_p = S_b / C_f \quad (3)$$

***The imprinting factor (I.F.):** The value is determined by the ratio of the partition coefficient of a substrate on the molecularly imprinted polymer ($K_{p\ MIP}$) to that on the non-imprinted polymer ($K_{p\ NIP}$), both prepared using the same monomer formulation (Eq. (4)) [20, 30]:

$$I.F. = K_{p,MIP} / K_{P,NIP} K_p = S_b / C_f \quad (4)$$

***Gibbs free energy of interaction (ΔG):** The free energy of substrate binding by MIP is determined using the equation [30]:

$$\Delta G = - RT\ Ln\ K_p \quad (5)$$

Tables 3-5 are shown the results of selectivity study by 0.2 grams of MIP and NIP samples were placed in 10 ml of each of 15 mg L^{-1} nitrophenol, phenol and *m*-cresol solutions in a shaker and left for 24 hrs. with mixing for certain periods at a speed of 50 rpm. Then the selectivity was measured after filtering the solutions, and the same was true for the rest of the samples [20].

Table 3. Selectivity study of MIP_{ONP} and NIP_{ONP} towards phenol and *m*-cresol

MIP_{ONP}	K_d (MIP) mg g^{-1}	K_d (NIP) mg g^{-1}	K (MIP)	K (NIP)	k'
ONP	0.129	0.112	-	-	-
phenol	0.063	0.0005	2.048	224	0.009
m-cresol	0.130	0.0005	0.992	224	0.004

Table 4. Selectivity study of MIP_{MNP} and NIP_{MNP} towards phenol and *m*-cresol

MIP_{MNP}	K_d (MIP) mg/g	K_d (NIP) mg/g	K (MIP)	K (NIP)	k'
MNP	0.623	0.589	-	-	-
phenol	0.285	0.0005	2.186	1178	0.002
***m*-cresol**	0.143	0.0005	4.357	1178	0.004

Table 5. Selectivity study of MIP_{PNP} and NIP_{PNP} towards phenol and *m*-cresol

MIP_{PNP}	K_d (MIP) mg/g	K_d (NIP) mg/g	K (MIP)	K (NIP)	k'
PNP	0.121	0.009	-	-	-
phenol	0.285	0.0005	0.425	18	0.024
***m*-cresol**	0.088	0.0005	1.375	18	0.076

The selectivity of MIP and NIP towards various templates was evaluated using mixed target compounds, ONP/ phenol, ONP/ *m*-cresol, MNP/ phenol, MNP/ *m*-cresol, PNP/ phenol, PNP/ *m*-cresol for the nine templates respectively.

The effect of molecular imprinting on selectivity was determined using the following relation [32]:

$$K_d = \frac{(C_i - C_f)}{W_p} \times V \quad (6)$$

where, K_d is the distribution coefficient, C_i and C_f are the initial and final concentrations of the analyte, W_p is the weight of the MIP, and V is the volume.

The selectivity coefficient (K) of the template in the presence of structurally similar molecules can be calculated as:

$$k = \frac{\text{Kd(nitrophenol)}}{\text{Kd(phenol or } m-\text{cresol)}} \quad (7)$$

The relative selectivity coefficient (k') is defined as the ratio of the selectivity coefficients of MIP and NIP [20]:

$$K` = K_{MIP} - K_{NIP} \quad (8)$$

Nitrophenols are ubiquitous environmental pollutant. To evaluate the efficiency of extracting the three studied nitrophenol pollutants from the aqueous solution. 45 ml of the three prepared aqueous nitrophenol solutions were taken and placed in a separating funnel. 5 ml of chloroform solution was added and shaken for ten minutes. The solutions were then left to separate the organic and aqueous layers. Then the chloroform layer was removed and the second and third extractions were repeated in the same way for all three solutions. The concertation of the aqueous nitrophenol solution was measured after each extraction.

The extraction process was repeated for acidic solutions at a pH =2 and for basic solutions at a pH =10, as indicated in Table 6 and Table 7. The point of choosing these pH values is because pKa value of the *ortho*, *meta*, and *para* nitrophenol are 7.23, 8.35, and 7.15, respectively [33-35]. Therefore, checking the effect of extraction at pH fewer and higher than the pKa will help in explaining the effect of protonation on the extraction efficiency.

Since the volume of the organic layer is not equal to the volume of the aqueous layer, the value of D, the distribution ratio was defined as the ratio of the concentration of a compound in the organic phase to that in the aqueous phase, was calculated from the first extraction efficiency for each acidity function from the following mathematical relationship as follows [36]:

$$D = \frac{Corg.}{Caq.} \quad (9)$$

where, $C_{org.}$ is the concentration of the remaining substance in the aqueous layer after the first extraction, $C_{aq.}$ is the concentration of the original substance in the aqueous layer [36].

Then it is possible to know the volume of the organic layer, the chloroform layer, required for any volume of the aqueous layer contaminated with nitrophenols, with high efficiency, using the following mathematical relationship [36]:

$$\%E = \frac{100D}{D + (\frac{Vaq.}{Vorg.})} \quad (10)$$

where %E it is the percentage of extraction efficiency, D distribution ratio, $V_{org.}$ The size of organic layer, $V_{aq.}$ The size of aqueous layer [36].

Table 6 presents the neutral isomers of nitrophenol, which exhibit lower degrees of ionization compared to the acidic isomers listed in Table 7. The ionized forms demonstrate reduced solubility in organic solvents, leading to decreased distribution ratios and extraction efficiencies. In contrast, at pH 2 an acidic aqueous environment all isomers predominantly exist in their neutral forms. These neutral species have limited solubility in aqueous media but exhibit enhanced solubility in organic solvents such as chloroform. Consequently, higher distribution ratios and extraction efficiencies are anticipated due to favorable partitioning into the organic phase.

Table 6. Concentrations of nitrophenol isomers before and after three extraction cycles at pH= 7

Nitrophenol Isomers	Initial C mg L^{-1}	Final C mg L^{-1}	%E	D
ONP, 1st E	15.0	1.0	93.3	14.0
ONP, 2nd E	-	0.3	98.0	
ONP, 3rd E	-	0.3	98.0	
MNP, 1st E	15.0	9.5	36.7	0.6
MNP, 2nd E	-	6.9	54.0	
MNP, 3rd E	-	4.0	73.3	
PNP, 1st E	15.0	10.9	27.3	0.4
PNP, 2nd E	-	0.3	98.0	-
PNP, 3rd E	-	0.2	98.7	-

At pH = (7 and 2), all nitrophenol isomers are predominantly in their protonated (neutral) forms. This is due to the fact that their pKa values are above 7, indicating that at this acidic pH, the compounds remain largely undissociated. Consequently, their solubility in aqueous solutions is low, and they are more readily extracted into organic solvents like chloroform [37].

Table 7. Concentrations of nitrophenol isomers before and after three extraction cycles at pH= 2

Nitrophenol Isomers	Initial C mg L^{-1}	Final C mg L^{-1}	%E	D
ONP, 1st E	15.0	0.7	95.3	20.4
ONP, 2nd E	-	0.4	97.3	-
ONP, 3rd E	-	0.2	98.7	-
MNP, 1st E	15.0	14.6	2.7	4.6
MNP, 2nd E	-	12.6	16.0	-
MNP, 3rd E	-	8.9	40.7	-
PNP, 1st E	15.0	9.2	38.7	0.6
PNP, 2nd E	-	5.8	61.3	-
PNP, 3rd E	-	0.0	100.0	-

At pH = 10, all three isomers are predominantly deprotonated, existing as phenoxide anions (Table 8). This deprotonation significantly alters their solubility characteristics. Phenoxide ions are highly soluble in aqueous solutions but have poor solubility in organic solvents like chloroform. As a result, the distribution of these compounds between the aqueous and organic phases is less favorable for extraction at this basic pH [37].

Table 8. Concentrations of nitrophenol isomers before and after three extraction cycles at pH= 10

Nitrophenol Isomers	Initial C mg L^{-1}	Final C mg L^{-1}	%E	D
ONP, 1st E	15.0	13.8	8.0	0.09
ONP, 2nd E	-	13.9	7.3	-
ONP, 3rd E	-	13.5	10	-
MNP, 1st E	15.0	15.0	0.0	0.0
MNP, 2nd E	-	15.0	0.0	-
MNP, 3rd E	-	14.7	2.0	-
PNP, 1st E	15.0	13.8	8.0	0.09
PNP, 2nd E	-	13.9	7.3	-
PNP, 3rd E	-	14.1	6.0	-

As presented in Table 8, all isomers are predominantly ionized. Extraction at pH higher than the pKa (nitrophenols are

deprotonated) shows a fewer efficiency, as expected. In addition, the ionized nature of these isomers leads to poor solubility in organic solvents, thereby resulting in low distribution ratios and reduced extraction efficiencies. Thus, it is highly recommended using acidic medium when extracting nitrophenols from aqueous solutions.

Analysis of the data presented in the Tables 6 and 7 indicates that a decrease in the pH corresponds to an increase in the D values. Specifically, for MNP, the D value at pH of 2 was 4.6, representing a more than sevenfold increase compared to the value of 0.6 observed at a neutral pH of 7. Whereas, at higher pH value, the extraction efficiency significantly declined (Figure 8).

4. CONCLUSIONS

MIPs were successfully synthesized using a template–monomer complex strategy, leading to the formation of highly specific binding sites within the polymer matrix. These sites exhibited strong affinity for the target nitrophenol isomers, demonstrating the effectiveness of the imprinting process in enhancing selectivity and recognition. The prepared MIP found to be selective, thermally stable and effectively suitable for removing nitrophenol isomers from acidic or neutral aqueous environments. The outcomes of this study are very helpful in the remediation of environments of nitrophenol pollution. The results also highlight the need for further studies to improve extraction and thus, removal efficiency.

ACKNOWLEDGMENT

The authors would like to thank the Department of Chemistry, College of Science, and University of Basrah for their support. Also, the authors declare that they have no known competing financial interests or personal relationships that could have appeared to influence the work reported in this paper.

REFERENCES

[1] Subashchandrabose, S.R., Megharaj, M., Venkateswarlu, K., Naidu, R. (2012). P-nitrophenol toxicity to and its removal by three select soil isolates of microalgae: The role of antioxidants. Environmental Toxicology and Chemistry. 31(9): 1980-1988. https://doi.org/10.1002/etc.1931

[2] Tchieno, F.M.M., Tonle, I.K. (2018). p-Nitrophenol determination and remediation: An overview. Reviews in Analytical Chemistry, 37(2). https://doi.org/10.1515/revac-2017-0019

[3] Toxicological Profile for Nitrophenols. Agency for Toxic Substances and Disease Registry (US). https://www.ncbi.nlm.nih.gov/books/NBK601133/?utm_source=chatgpt.com.

[4] Al-Naiema, I.M., Stone, E.A. (2017). Evaluation of anthropogenic secondary organic aerosol tracers from aromatic hydrocarbons. Atmospheric Chemistry and Physics, 17(3): 2053-2065.

[5] Iinuma, Y., Brüggemann, E., Gnauk, T., Müller, K., et al. (2007). Source characterization of biomass burning particles: The combustion of selected European conifers, African hardwood, savanna grass, and German and Indonesian peat. Journal of Geophysical Research: Atmospheres, 112(D8). https://doi.org/10.1029/2006JD007120

[6] Olker, J.H., Elonen, C.M., Pilli, A., Anderson, A., et al. (2022). The ECOTOXicology knowledgebase: A curated database of ecologically relevant toxicity tests to support environmental research and risk assessment. Environmental Toxicology and Chemistry, 41(6): 1520-1539. https://doi.org/10.1002/etc.5324

[7] Zieris, F.J., Feind, D., Huber, W. (1988). Long-term effects of 4-nitrophenol in an outdoor synthetic aquatic ecosystem. Archives of Environmental Contamination and Toxicology, 17(2): 165-175. https://doi.org/10.1007/BF01056021

[8] Chen, G. (2004). Electrochemical technologies in wastewater treatment. Separation and Purification Technology, 38(1): 11-41. https://doi.org/10.1016/j.seppur.2003.10.006

[9] Fu, F., Wang, Q. (2011). Removal of heavy metal ions from wastewaters: A review. Journal of Environmental Management, 92(3): 407-418. https://doi.org/10.1016/j.jenvman.2010.11.011

[10] Crini, G., Lichtfouse, E. (2019). Advantages and disadvantages of techniques used for wastewater treatment. Environmental Chemistry Letters, 17(1): 145-155. https://doi.org/10.1007/s10311-018-0785-9

[11] Wulff, G. (1995). Molecular imprinting in cross-linked materials with the aid of molecular templates— A way towards artificial antibodies. Angewandte Chemie International Edition in English, 34(17): 1812-32. https://doi.org/10.1002/anie.199518121

[12] Chen, L., Wang, X., Lu, W., Wu, X., Li, J. (2016). Molecular imprinting: Perspectives and applications. Chemical Society Reviews, 45(8): 2137-211. https://doi.org/10.1039/C6CS00061D

[13] Haupt, K., Mosbach, K. (2000). Molecularly imprinted polymers and their use in biomimetic sensors. Chemical Reviews, 100(7): 2495-504. https://doi.org/10.1021/cr990099w

[14] Lang, D., Shi, M., Xu, X., He, S., Yang, C., Wang, L., et al. (2021). DMAEMA-grafted cellulose as an imprinted adsorbent for the selective adsorption of 4-nitrophenol. Cellulose, 28(10): 6481-98. https://doi.org/10.1007/s10570-021-03920-9

[15] Zakaria, N.D., Yusof, N.A., Haron, J., Abdullah, A.H. (2009). Synthesis and evaluation of a molecularly imprinted polymer for 2,4-dinitrophenol. International Journal of Molecular Sciences, 10(1): 354-365. https://doi.org/10.3390/ijms10010354

[16] Hashemi-Moghaddam, H., Abbasi, F. (2015). Synthesis of molecularly imprinted polymers coated on silica nanoparticles for removal of p-nitrophenol from crude pharmaceuticals. Pharmaceutical Chemistry Journal, 49(4): 280-286. https://doi.org/10.1007/s11094-015-1270-4.

[17] Mehdinia, A, Dadkhah, S., Baradaran Kayyal, T., Jabbari, A. (2014). Design of a surface-immobilized 4-nitrophenol molecularly imprinted polymer via pre-grafting amino functional materials on magnetic nanoparticles. J Chromatogr A, 1364: 12-19. https://doi.org/10.1016/j.chroma.2014.08.058

[18] Ersöz, A., Denizli, A., Şener, İ., Atılır, A., Diltemiz, S., Say, R. (2004). Removal of phenolic compounds with nitrophenol-imprinted polymer based on π–π and

hydrogen-bonding interactions. Separation and Purification Technology, 38(2): 173-179. https://doi.org/10.1016/j.seppur.2003.11.004

[19] Corona Rivera, M.A., Cisneros Covarrubias, C.A., Fernández Escamilla, V.V.A., Mendizábal Mijares, E., Pérez López, J.E. (2022). Synthesis and characterization of pH‐responsive water‐dispersed nanohydrogels of cross‐linked polyacrylamide‐co‐polyacrylic acid. Polymer Engineering & Science, 62(6): 1797-1810. https://doi.org/10.1002/pen.25965

[20] Kanai, T., Sanskriti, C., Vislawath, P., Samui, A.B. (2013). Acrylamide based molecularly imprinted polymer for detection of m-nitrophenol. Journal of Nanoscience and Nanotechnology, 13(4): 3054-3061. https://doi.org/10.1166/jnn.2013.7399

[21] Rifa'i, A., Hashim, S., Muhamad, I. (2015). Synthesis and characterization of poly (acrylamide-co-acrylic acid)-grafted-poly (styrene-co-methyl methacrylate) microgels by emulsion polymerization. Journal of Advanced Research in Materials Science, 8(1): 10-15.

[22] Jing, Z., Xu A, Liang, Y-Q., Zhang, Z., Yu, C., Hong, P., et al. (2019). Biodegradable poly (acrylic acid-co-acrylamide)/poly (vinyl alcohol) double network hydrogels with tunable mechanics and high self-healing performance. Polymers, 11(6): 952. https://doi.org/10.3390/polym11060952

[23] Hassan, M.F., Yusof, S.Z.M. (2014). Poly (acrylamide-co-acrylic acid)-zinc acetate polymer electrolytes: Studies based on structural and morphology and electrical spectroscopy. Microscopy Research, 2(2): 30-38. http://doi.org/10.4236/mr.2014.22005

[24] Hebeish, A., Elrafie, M., Rabie, A., Aly, A., Refaat, D. (2015). Synthesis and properties of superabsorbent carboxymethyl cellulose graft-poly (acrylic acid-co-acrylamide). Egyptian Journal of Chemistry, 58(6): 721-739.

[25] Gupta, I., Tomar, R.S., Nagpal, A., Singhal, R. (2006). Synthesis and characterization of poly (AAm-co-BMA-co-AAc) hydrogels: Effect of acrylamide content on swelling behaviour. Designed Monomers and Polymers, 9(6): 589-605. http://doi.org/10.1163/156855506778943993

[26] Topçu, A.A., Bereli, N., Albayrak, İ., Denizli, A. (2017). Creatinine imprinted poly (hydroxyethyl methacrylate)-based cryogel cartridges. Journal of Macromolecular Science, Part A, 54(8): 495-501. https://doi.org/10.1080/10601325.2017.1320756

[27] Grygoryeva, K., Kubecka, J., Pysanenko, A., Lengyel, J., Slavicek, P., Farnik, M. (2016). Photochemistry of nitrophenol molecules and clusters: Intra-vs intermolecular hydrogen bond dynamics. The Journal of Physical Chemistry A, 120(24): 4139-4146. https://doi.org/10.1021/acs.jpca.6b04459

[28] Vasapollo, G., Sole, R.D., Mergola, L., Lazzoi, M.R., Scardino, A., Scorrano, S., Mele, G. (2011). Molecularly imprinted polymers: Present and future prospective. International Journal of Molecular Sciences, 12(9): 5908-5945. https://doi.org/10.3390/ijms12095908

[29] Huang, X., Kong, L., Li, X., Zheng, C., Zou, H. (2003). Molecular imprinting of nitrophenol and hydroxybenzoic acid isomers: Effect of molecular structure and acidity on imprinting. Journal of Molecular Recognition, 16(6): 406-411. https://doi.org/10.1002/jmr.627

[30] Spivak, D.A. (2005). Optimization, evaluation, and characterization of molecularly imprinted polymers. Advanced Drug Delivery Reviews, 57(12): 1779-1794. https://doi.org/10.1016/j.addr.2005.07.012

[31] Sellergren, B., Shea, K.J. (1993). Influence of polymer morphology on the ability of imprinted network polymers to resolve enantiomers. Journal of Chromatography A, 635(1): 31-49. https://doi.org/10.1016/0021-9673(93)83112-6

[32] Duffy, D.J., Das, K., Hsu, S.L., Penelle, J., Rotello, V. M., Stidham, H.D. (2002). Binding efficiency and transport properties of molecularly imprinted polymer thin films. Journal of the American Chemical Society, 124(28): 8290-8296. https://doi.org/10.1021/ja0201146

[33] Ehlerova, J., Trevani, L., Sedlbauer, J., Tremaine, P. (2008). Spectrophotometric determination of the ionization constants of aqueous nitrophenols at temperatures up to 225°C. Journal of Solution Chemistry, 37: 857-874. https://doi.org/10.1007/s10953-008-9279-x

[34] Sajjadi, S.M. (2024). Simultaneous spectrophotometric quantification of 2-nitrophenol and 4-nitrophenol in binary mixtures based on partial least squares method: Comparison analysis of five types of data sets. Analytical and Bioanalytical Chemistry Research, 11(3): 327-334.

[35] Yang, B., Shi, T.-T., Hu, W.-G., Gao, G.-J., Liu, Y.-P., Yu, J.-G. (2025). S-containing graphene oxide composite for the adsorptive removal of p-nitrophenol from aqueous solutions. Molecules, 30(9): 2046. https://doi.org/10.3390/molecules30092046

[36] Harris, D.C., Lucy, C.A. (2019). Quantitative Chemical Analysis. https://books.google.iq/books?id=bVPHDwAAQBAJ.

[37] Koubaissy, B., Joly, G., Magnoux, P. (2008). Adsorption and competitive adsorption on zeolites of nitrophenol compounds present in wastewater. Industrial & Engineering Chemistry Research, 47(23): 9558-9565. https://doi.org/10.1021/ie8001777